

Preparation of Anatase TiO₂ Thin Films with (OⁱPr)₂Ti(CH₃COCHCONEt₂)₂ Precursor by MOCVD[†]

Byoung-Jae Bae, Kwangyeol Lee,[‡] Won Seok Seo, Md. Arzu Miah, Keun-Chong Kim,[§] and Joon T. Park*

National Research Laboratory, Department of Chemistry and School of Molecular Science (BK21),
Korea Advanced Institute of Science and Technology (KAIST), Daejeon 305-701, Korea

[‡]Department of Chemistry, Korea University, Seoul 136-701, Korea

[§]Department of Management Information System, College of Business Management,
Hong-Ik University, Chochiwon, Chungnam 339-701, Korea

Received April 6, 2004

The reaction of titanium tetraisopropoxide with 2 equiv of *N,N*-diethyl acetoacetamide affords Ti(OⁱPr)₂(CH₃COCHCONEt₂)₂ (**1**) as colorless crystals in 80% yield. Compound **1** is characterized by spectroscopic (Mass and ¹H/¹³C NMR) and microanalytical data. Molecular structure of **1** has been determined by a single crystal X-ray diffraction study, which reveals that it is a monomeric, *cis*-diisopropoxide and contains a six coordinate Ti(IV) atom with a *cis*(CONEt₂), *trans*(COCH₃) configuration (**1a**) in a distorted octahedral environment. Variable-temperature ¹H NMR spectra of **1** indicate that it exists as an equilibrium mixture of *cis*, *trans* (**1a**) and *cis*, *cis* (**1b**) isomers in a 0.57 : 0.43 ratio at -20 °C in toluene-*d*₈ solution. Thermal properties of **1** as a MOCVD precursor for titanium dioxide films have been evaluated by thermal gravimetric analysis and vapor pressure measurement. Thin films of pure anatase titanium dioxide (after annealing above 500 °C under oxygen) have been grown on Si(100) with precursor **1** in the substrate temperature range of 350-500 °C using a bubbler-based MOCVD method.

Key Words : Titanium dioxide (TiO₂), Thin films, MOCVD, Ti precursor, β-Keto amide ligand

Introduction

In recent years, titanium dioxide (TiO₂) and perovskite titanates (Ba_xSr_{1-x}TiO₃ (BST) and PbZr_xTi_{1-x}O₃ (PZT)) have attracted considerable attention for their practical application as capacitor materials in next generation computer memory devices.¹⁻⁶ For the preparation of thin films of these materials, the metal-organic chemical vapor deposition (MOCVD) offers both technical and economical advantages such as a conformal step coverage, easy composition controllability, large area deposition capability, and a high deposition rate.⁷⁻¹⁰ An essential requirement for a successful MOCVD is the availability of suitable metal-organic precursors with sufficient volatility and thermal stability for gas-phase transport to the deposition site and with clean decomposition pathways to produce the desired materials.

Thin films of TiO₂ and related oxides have been commonly obtained by MOCVD using Ti(OⁱPr)₄ in the presence of oxygen.¹¹⁻¹³ Alkoxide precursors, however, contain unsaturated Ti centers, which makes them highly reactive to air and moisture and susceptible to pre-reaction in MOCVD reactors with oxygen or other precursors. To overcome these problems, modified alkoxides of titanium with an increased coordinative saturation at the metal center, such as Ti(tmhd)₂(OⁱPr)₂ and Ti(tmhd)₂(mpd) (tmhd = 2,2,6,6-tetramethylheptane-3,5-dionate, mpd = 2-methyl-2,4-pentanedioxy), have been investigated as alternative precursors.¹⁴⁻²⁰ NMR studies of

these complexes have confirmed that they do not pre-react with other MO precursors employed in the preparation of perovskite titanate films. A functionalized alkoxide or β-keto iminate ligand can also increase the coordinative saturation by providing an additional Lewis base site to form chelate rings.²¹⁻²⁴

In multi-component oxide growth for BST and PZT materials, the precursors need to have similar vaporization temperatures, and should deposit oxides in a similar temperature region, in order to achieve a good layer uniformity and control of the stoichiometry and to avoid build-up of residue in the evaporator. Most oxide precursors, however, have been limited to metal alkoxides or β-diketonates.²⁵ We herein report synthesis and characterization of Ti(OⁱPr)₂(CH₃COCHCONEt₂)₂ (**1**) precursor with β-keto amide ligands, and growth of TiO₂ thin films by MOCVD of **1**.

Experimental Section

General techniques. All manipulations were carried out by using standard Schlenk techniques and Vacuum Atmospheres HE-439 drybox under a dry, oxygen-free argon atmosphere. All solvents were dried according to standard procedures, distilled under argon, and stored over 4 Å molecular sieves. The following chemicals were obtained from commercial sources and used as received: *N,N*-diethyl acetoacetamide (Acros); Ti(OⁱPr)₄ (Aldrich). The ¹H-NMR (400 MHz) and ¹³C-NMR (100 MHz) spectra were recorded on a Bruker AVANCE-400 spectrometer. The melting point was measured using an electrothermal melting point

[†]Dedicated to Professor Yong Hae Kim for his distinguished achievements in organic chemistry.

*Corresponding Author. e-mail: joontpark@kaist.ac.kr

apparatus in a sealed capillary under argon and is given uncorrected. Mass spectral data were obtained on a JEOL SX-102A instrument operating in electron impact (EI) mode. Elemental analysis was performed by the staff of the Energy and Environment Research Center at KAIST. Thermal analysis was carried out using a TA TGA 2050 and TA DSC 2010 under nitrogen atmosphere with 10 sccm flow and 10 °C/min heating rate. Equilibrium vapor pressure measurement for **1** was carried out over a temperature range of 60–140 °C according to the method reported in the literature.²⁶ The crystallinity of films was examined by X-ray diffraction (XRD) measurements using Rigaku D/MAX-RC 12 kW diffractometer with Cu K α radiation. The surface morphology, fractured sections, and the thickness of the films were checked by scanning electron microscopy (SEM, JEOL JSM 840A). The atomic composition of the film was determined by using Rutherford backscattering spectroscopy (RBS, NEC 3SDH) and Auger electron spectroscopy (AES, SAM 4300). Film adherence was tested by Scotch tape peeling.

Synthesis of complex 1. *N,N*-Diethyl acetoacetamide (5.64 g, 35.9 mmol) was added dropwise to Ti(O^{*i*}Pr)₄ (5.08 g, 17.9 mmol) at room temperature. The reaction mixture was stirred for 1 h, and the volatiles were removed under reduced pressure. Recrystallization of the white residue in toluene at –30 °C afforded **1** (6.87 g, 14.3 mmol, 80%) as colorless crystals: MS (70 eV) *m/z* 419 [M–C₃H₇O]⁺. Anal. Calc. for C₂₂H₄₂N₂O₆Ti: C, 55.23; H, 8.85; N, 5.86. Found: C, 55.73; H, 8.41; N, 6.07%.

Cis, trans isomer **1a**: m.p. 63–65 °C; ¹H NMR (toluene-*d*₈, –20 °C): δ 5.14 (m, 2H, OCH(CH₃)₂), 4.83 (s, 2H, CH), 2.91, 2.55 (q, 4H each, NCH₂CH₃), 1.92 (s, 6H, CH₃), 1.44, 1.34 (d, 6H each, OCH(CH₃)₂), 0.88, 0.68 (t, 6H each, NCH₂CH₃). ¹³C NMR (toluene-*d*₈, –20 °C): δ 179.7, 168.2 (CO), 86.3 (CH), 42.0, 41.0 (NCH₂CH₃), 26.0 (CH₃), 25.9, 25.6 (OCH(CH₃)₂), 13.7, 13.6 (NCH₂CH₃).

Cis, cis isomer **1b**: m.p. 73–74 °C; ¹H NMR (toluene-*d*₈, –20 °C): δ 5.22, 5.09 (m, 1H each, OCH(CH₃)₂), 4.87, 4.79 (s, 1H each, CH), 2.98, 2.62 (2q, 4H each, NCH₂CH₃), 1.87, 1.78 (s, 3H each, CH₃), 1.44–1.29 (d, 3H each, OCH(CH₃)₂), 1.05–0.68 (t, 6H each, NCH₂CH₃). ¹³C NMR (toluene-*d*₈, –20 °C): δ 182.1, 182.0, 179.7, 168.5 (CO), 86.7, 84.5 (CH), 42.4, 42.1, 41.3, 41.0 (NCH₂CH₃), 26.7, 25.9 (CH₃), 26.2, 26.0, 25.8, 25.6 (OCH(CH₃)₂), 14.0, 13.7, 13.6, 13.5 (NCH₂CH₃).

X-Ray crystallographic study of 1a. Crystals of **1a** suitable for X-ray study were obtained by recrystallization in toluene at –30 °C. A colorless crystal was mounted in thin-walled glass capillary under an argon atmosphere, and the capillary was temporarily sealed with silicon grease and then flame-sealed. The determination of unit cell parameters and the orientation matrix and the collection of intensity data were made on an Enraf-Nonius CAD-4 diffractometer utilizing graphite-monochromated Mo-K α radiation. Lorentz and polarization corrections were applied to the intensity data while no absorption correction was applied. Intensities of three standard reflections monitored every 4 h showed no significant decay over the course of data collection. Relevant

Table 1. Crystallographic data for **1a**

Formula	C ₂₂ H ₄₂ N ₂ O ₆ Ti
Fw	478.48
Cryst syst	Monoclinic
Space group	<i>P</i> 2 ₁ / <i>a</i>
<i>a</i> [Å]	17.066(3)
<i>b</i> [Å]	17.633(9)
<i>c</i> [Å]	9.599(1)
β [°]	103.36(1)
Volume [Å ³]	2810.2(16)
Z	4
D _{calc} [Mg m ^{–3}]	1.131
μ [mm ^{–1}]	0.338
Cryst size [mm ³]	0.59 × 0.30 × 0.20
θ ranges	2.18 to 20.00°
Index ranges	0 ≤ <i>h</i> ≤ 16, 0 ≤ <i>k</i> ≤ 16, –9 ≤ <i>l</i> ≤ 8
Rflns collected	2733
Indepdt rflns	2620 (<i>R</i> _{int} = 0.0539)
Data/restraints/params	2620/0/261
Goodness-of-fit on <i>F</i> ²	1.046
Final <i>R</i> indices on <i>F</i> ² (<i>I</i> > 2 σ (<i>I</i>))	<i>R</i> ₁ = 0.0793, <i>R</i> _w = 0.1001
<i>R</i> indices on <i>F</i> ² (all data)	<i>R</i> ₁ = 0.1188, <i>R</i> _w = 0.1537
D(<i>r</i>) and hole [eÅ ^{–3}]	0.468 and –0.593

crystallographic details are shown in Table 1. All calculations were performed using the SHELXS-86 and SHELXL-93 computer programs.^{27,28} Scattering factors for all atoms were included in the software package. The structure of **1a** was solved using a combination of Patterson and Fourier map and refined by the full-matrix least-squares technique with anisotropic thermal parameters for all non-hydrogen atoms. All hydrogen atoms were placed in calculated positions and included in the structure factor calculation. Crystallographic data (excluding structure factor) for the structure of **1a** have been deposited with the Cambridge Crystallographic Data Center (CCDC) as supplementary publication number CCDC 184681.

MOCVD experiment. Thin films of TiO₂ were deposited onto 2.0 × 1.0 cm² (100) silicon substrates in a vertical cold-wall reactor as shown in Figure 1. Precursor was loaded into a stainless steel vessel in a drybox, and introduced into the system through a 1/4 inch stainless steel tube, whose end was approximately 2.0 cm above the surface of substrate. Dioxygen was introduced into the reaction chamber and the precursor was introduced by passing Ar carrier gas of 7 sccm through a bubbler which was kept at constant temperature of 100 °C. The gas line leading to the CVD chamber was heated and maintained at *ca.* 130 °C to avoid condensation of

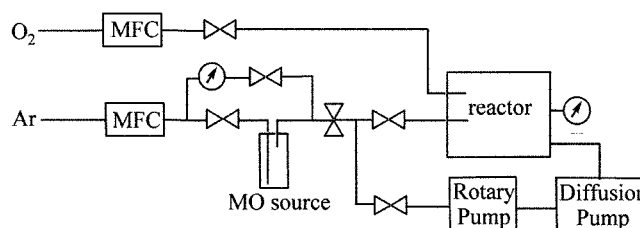


Figure 1. Schematic diagram of the vertical cold-wall MOCVD system.

the precursor. Flow rate of the precursor was controlled by adjusting the conductance of the fine metering valve located between the bubbler and the reaction chamber, and was monitored by a Pirani gauge in the deposition chamber. The substrate temperature was provided by passing an electric current through the substrate, monitored using an optical pyrometer, and adjusted to the desired value. TiO₂ films were deposited over a range of substrate temperatures from 350 to 500 °C for 1 h with varying flow rates, while other deposition parameters were fixed. After deposition, films were annealed in oxygen atmosphere at 500 °C for 1 h.

Results and Discussion

Synthesis and characterization of precursor 1. The neat reaction of titanium tetraisopropoxide with 2 equiv of *N,N*-diethyl acetoacetamide produces monomeric Ti(O^{*i*}Pr)₂(CH₃COCHCONEt₂)₂ (**1**) in 80% yield. Formulation of **1** is supported by the observation of the [MO^{*i*}Pr]⁺ ion in EI mass spectrum and by microanalytical data.

The X-ray structural characterization of **1** (vide infra) shows *cis*(O^{*i*}Pr), *cis*(CONEt₂), *trans*(COCH₃) configuration (**1a**) of the ligand arrangement. This complex in solution may exist in three diastereomeric forms (**1a-1c**) as shown in Scheme 1, assuming that the two isopropoxide groups maintain the *cis* configuration.²⁹ The stability of the *cis*-alkoxide isomer has been ascribed to the oxygen (p) → metal (d) π-bonding; in the *cis*-isomer all three d_π orbitals of titanium are involved whereas in the *trans*-isomer only two of the d_π orbitals can participate.³⁰ The *cis*, *trans* (**1a**) and *trans*, *cis* (**1c**) diastereomers possess C₂-symmetry, and thus both have only one environment for each of OCNEt₂, OCCH₃, -CH=, and O^{*i*}Pr groups. The *cis*, *cis* (**1b**) isomer has C₁ symmetry and consequently contains two inequivalent OCNEt₂, OCCH₃, -CH=, and O^{*i*}Pr moieties with diastereotopic methyl groups of the O^{*i*}Pr moiety and a restricted rotation of the OC-NEt₂ bond.

Variable temperature (VT) ¹H NMR spectra of **1** (400 MHz, toluene-*d*₈) are shown in Figure 2. The limiting low temperature spectrum at -20 °C reveals that **1** exists as an equilibrium mixture of **1a** and **1b** diastereomers in a ratio of 0.57 : 0.43. The structurally characterized isomer **1a** is assumed to be the major isomer, although the general features of ¹H NMR spectra of **1a** and **1c** are expected to be

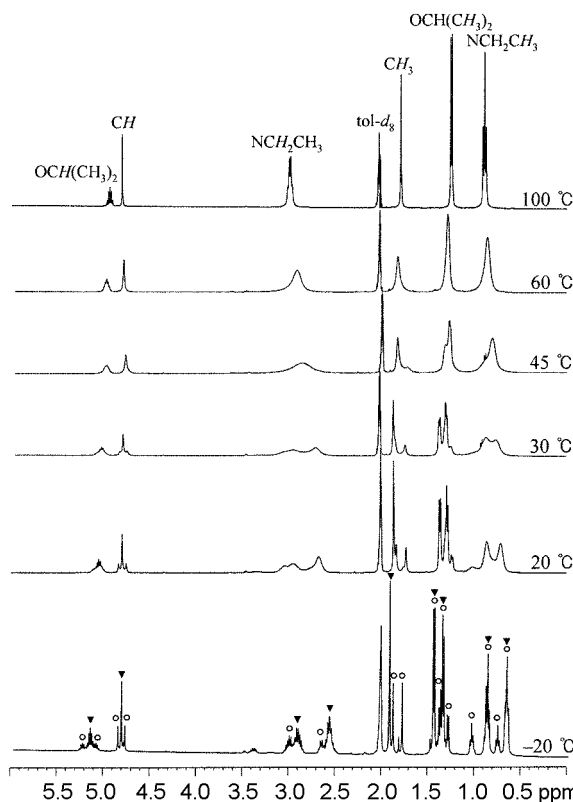
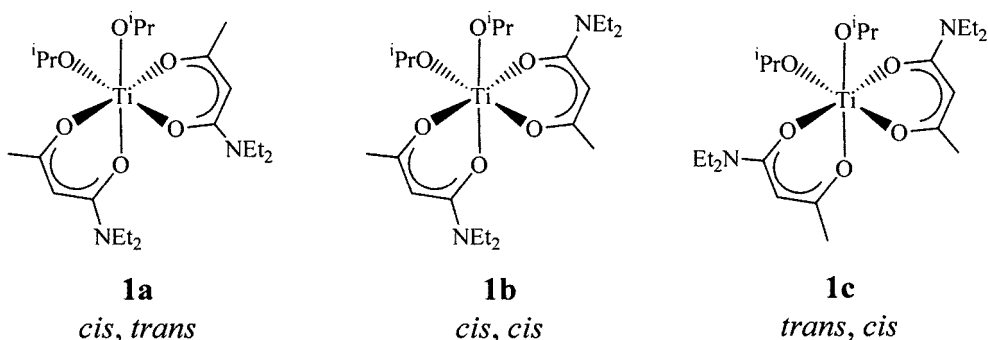


Figure 2. Variable temperature ¹H NMR spectra (400 MHz, toluene-*d*₈) of a mixture of **1a** (▼) and **1b** (○).

similar. The two doublets at δ 1.44 and 1.34 (denoted as ▼) are due to the geminal methyl protons of isopropoxide groups in **1a**. Four doublets are expected for the same protons of **1b**, but only two doublets at δ 1.38 and 1.29 (denoted as ○) are clearly seen and the rest are overlapped with the resonances of **1a**. Methyne protons of the isopropoxide group appear as multiplets in the region of δ 5.1-5.3. A singlet at δ 4.83 (denoted as ▼) and a pair of singlet at δ 4.87 and 4.79 (denoted as ○) are assigned to the chelate ring -CH= protons of **1a** and **1b**, respectively. A singlet at δ 1.92 (**1a**, denoted as ▼) and two singlets at δ 1.87 and 1.78 (**1b**, denoted as ○) are due to the methyl groups on the chelate ring. Methyl protons of the NEt₂ moieties appear as two triplets (denoted as ▼) at δ 0.88 and 0.68 for **1a** and four triplets (denoted as ○) in the range of δ 0.6-1.1 for **1b** overlapped with **1a** resonances, which are



Scheme 1. *Cis*-isopropoxide isomers of **1**.

due to a restricted rotation of the OC-NEt₂ bond. Multiplet patterns in the δ 2.4–3.1 range are attributed to the methylene protons of the NEt₂ groups. These ¹H NMR peak assignments have been confirmed by the decoupling experiment and by the 2D ¹H-¹H and ¹H-¹³C COSY spectra. As the temperature increases, all the resonances broaden to the same extent, coalesce, and reveal time-averaged single resonance for each kind of protons at 100 °C (top spectrum in Figure 2). The diastereomerization for various *cis* Ti(β -diketonate)₂(OR)₂ complexes has been previously suggested to occur by a twist mechanism without bond rupture, which involves a trigonal

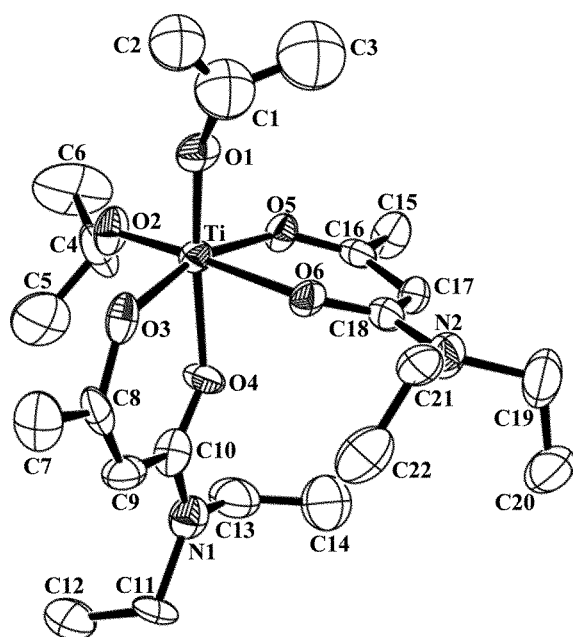


Figure 3. Molecular structure and atomic labeling scheme for **1a** with 20% thermal ellipsoid probability. All hydrogen atoms are omitted for clarity.

Table 2. Selected bond lengths [Å] and angles [°] for **1a**

Bond Lengths			
Ti-O(1)	1.770(11)	Ti-O(2)	1.774(13)
Ti-O(3)	1.997(12)	Ti-O(4)	2.025(12)
Ti-O(5)	1.950(11)	Ti-O(6)	2.034(11)
O(1)-C(1)	1.487(11)	O(2)-C(4)	1.40(3)
O(3)-C(8)	1.36(2)	O(4)-C(10)	1.26(2)
O(5)-C(16)	1.26(2)	O(6)-C(18)	1.26(2)
N(1)-C(10)	1.32(2)	N(2)-C(18)	1.38(2)
Bond Angles			
O(1)-Ti-O(2)	98.2(5)	O(1)-Ti-O(3)	91.8(5)
O(1)-Ti-O(4)	170.0(5)	O(1)-Ti-O(5)	100.1(5)
O(1)-Ti-O(6)	89.0(5)	O(2)-Ti-O(3)	99.5(5)
O(2)-Ti-O(4)	91.3(6)	O(2)-Ti-O(5)	90.4(5)
O(2)-Ti-O(6)	170.9(5)	O(3)-Ti-O(4)	83.2(5)
O(3)-Ti-O(5)	163.2(5)	O(3)-Ti-O(6)	85.6(4)
O(4)-Ti-O(5)	83.1(4)	O(4)-Ti-O(6)	81.9(4)
O(5)-Ti-O(6)	81.9(4)	C(10)-N(1)-C(11)	126.5(19)
C(10)-N(1)-C(13)	118.3(18)	C(11)-N(1)-C(13)	114.8(18)
C(18)-N(2)-C(19)	123.4(18)	C(18)-N(2)-C(21)	120.8(15)
C(19)-N(2)-C(21)	115.0(18)		

prismatic transition.³¹

Molecular structure of 1. The molecular structure of **1** is shown in Figure 3 and important bond lengths and angles are summarized in Table 2. The crystal structure reveals that only *cis*(OCNEt₂), *trans*(OCCH₃) isomer (**1a**) exists in the solid state. This arrangement appears to be the favored configuration for an octahedral complex of the type *cis*-M(AB)₂X₂, because only *cis*(N), *trans*(O) isomer has been found in previous studies for Ti(oxinate)₂(2,6-(ⁱPr)₂C₆H₃O)₂ and Ti(8-quinolinolate)₂(2,6-(ⁱPr)₂C₆H₃O)₂ in both solid and solution states.^{32,33} The titanium ion is hexa-coordinated with a distorted octahedral geometry. The Ti-O bond lengths fall into two distinct classes of longer Ti-O(β -keto amide) bonds [Ti-O(3), Ti-O(4), Ti-O(5), and Ti-O(6); av. 2.002(12) Å] and shorter Ti-O(OⁱPr) bonds [Ti-O(1) and Ti-O(2); av. 1.772(12) Å]. The long Ti-O bonds are comparable to those in Ti-O(β -diketonate) of [Ti(OⁱPr)₃(tmhd)]₂ (av. 2.060(9) Å), but short Ti-O bonds are exceptionally shorter than the Ti-O(alkoxide) of tmhd complex (av. 1.920(9) Å).³⁴ This can be accounted for by the strong *trans* influence of CONEt₂ group in the β -keto amide, which serves as a good electron-donating group. The two β -keto amide rings are planar with typical C-C and C-O bond lengths. The angle between short Ti-O bonds is ca. 100° and that between long bonds is ca. 80°. The bite angles of the β -keto amide ligand are 81.9(4)° and 83.2(5)°, close to the β -diketonate bite angle of 80.53(4)° in [Ti(OⁱPr)₃(tmhd)]₂. The NEt₂ planes are nearly co-planar with the β -keto amide ring (dihedral angle = 2.1(7)° and 1.5(8)°), and thus forming an extended conjugated system; the electron density of the lone pairs of nitrogen atoms of CONEt₂ group is delocalized into the β -keto amide ring, leading to significant resonance stabilization of the chelating metal-oxygen bonds. This type of resonance stabilization of the chelate ring may increase the thermal stability of precursors.³⁵

Vapor pressure measurement and stability study. In order to optimize the temperature at which the precursor vaporizes during the CVD process, the equilibrium vapor pressures of **1** are measured in the temperature range of 65–140 °C. The data were fit by a simple linear least-squares analysis, and Clausius-Clapeyron equation can be expressed as $\log P$ (Torr) = 4.423–1466/*T* (333 < *T* < 413 K, *r*² = 0.989). The vapor pressure exceeded 3 Torr at 100 °C, a temperature well within the acceptable range for normal CVD evaporator systems. The value of vaporization enthalpy $\Delta H_{\text{vap}}^{\circ}$ was assumed to be constant over these ranges and determined to be 28.07 kJ mol⁻¹. Similar expression of $\log P$ (Torr) = 11.96 – 5165/*T* (353 < *T* < 413 K; $\Delta H_{\text{vap}}^{\circ}$ = 98.61 kJ mol⁻¹) is reported for Ti(tmhd)₂(OⁱPr)₂.¹⁴

The thermal stability of **1** was investigated by thermal gravimetric analysis (TGA) and differential scanning calorimetry (DSC) at the atmospheric pressure (carrier gas: N₂, heating rate: 10 °C/min). The TGA and DSC traces are illustrated in Figure 4. The sharp endothermic peak in the DSC curves correlates well with the melting point estimated by the visual method. In the TGA, a single weight loss step was observed with an onset temperature of 180 °C and

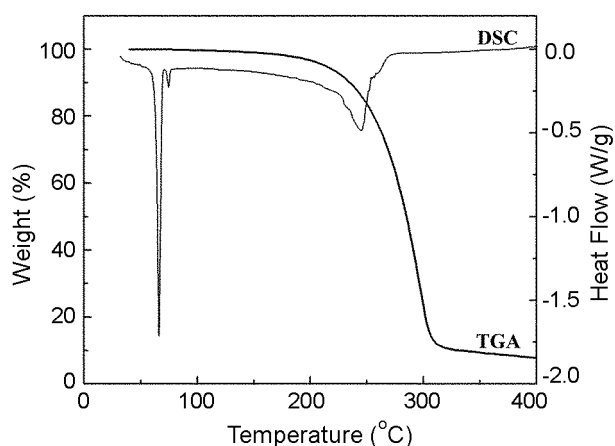


Figure 4. Ambient pressure TGA (thick line) and DSC (thin line) plots for **1**. (N₂ flow, 10 sccm, 10 °C/min).

completion at 440 °C. In this temperature range, 95 ± 2% of **1** vaporizes into the gas phase, leaving a small carbonaceous residue ($T_{50} = 285$ °C; residue = 6.5%), which is comparable to that ($T_{50} = 250$ °C; residue = 3.7%) of Ti(tmhd)₂(O^{*i*}Pr)₂.

Preparation of TiO₂ thin films using **1** by MOCVD.

The variable-temperature NMR studies have confirmed that precursor **1** do not pre-react with other MO precursors such as Pb(tmhd)₂ or Sr(tmhd)₂ in toluene-*d*₈ up to 100 °C. Compound **1** melts at 63–74 °C and exists as a liquid phase with sufficient vapour pressure at the evaporation temperature (3.1 Torr at 100 °C), and shows no significant decomposition upon prolonged heating. To examine the decomposition characteristics of **1**, TiO₂ film growth was carried out on Si(100) substrates by conventional bubbler-based MOCVD method. The vertical cold-wall reactor was used in the temperature range 350–500 °C as shown in Figure 1. Typical run time was 1 h, resulting in films with a thickness of 80, 105, 140 and 180 Å at 350, 400, 450 and 500 °C, respectively. The logarithm of the deposition rate is plotted against the reciprocal of the absolute temperature, and the slope of the plot gives activation energy of about 1.41 eV. The deposition rate at each deposition temperature can be doubled by doubling the feed-rate of the precursor (argon gas flow), implying that the film growth is mass-transport controlled.

The crystallinity of deposited films was examined by X-ray diffraction (XRD). The as-deposited films show no diffraction peaks of crystalline TiO₂ phase even up to a deposition temperature of 500 °C, presumably, due to either low deposition temperatures or strong deviation from the stoichiometric O/Ti ratio. When the films were annealed for 1 h under oxygen above 500 °C, the original amorphous films became crystalline pure anatase TiO₂ (the crystallinity improved with increasing annealing temperature).^{36,37} The X-ray diffraction pattern of anatase TiO₂ thin film (thickness 145 nm) is shown in Figure 5(a). The XRD peaks (Cu Kα) at 25.3°, 37.8°, 48.0°, and 55.0° correspond to anatase (101), (004), (200) and (211) planes, respectively. The FWHM value of 0.18° for the (101) peak corresponds to approximate crystallite size of 50 nm from the Scherrer equation.³⁸ The growth of polycrystalline TiO₂ with an anatase phase was

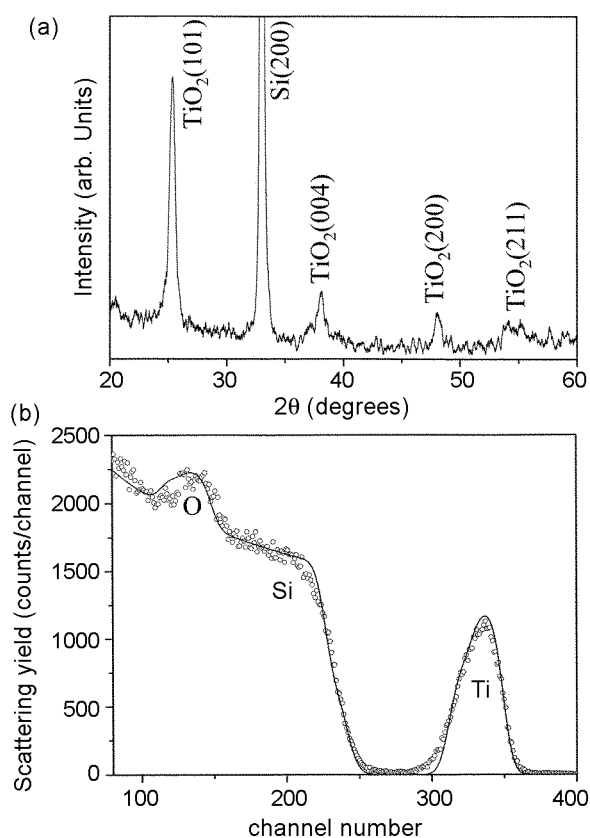


Figure 5. (a) X-ray diffraction pattern for a 145 nm TiO₂ film on Si(100) deposited at 450 °C and annealed at 500 °C; (b) A backscattering spectrum for 2.24 MeV ⁴He⁺ ions incident on a TiO₂ film on a silicon substrate. The dotted curve represents the experimental spectrum and the solid lines are computer fitted theoretical signals with a O/Ti ratio of 2.3. The scattering angle was 165°.

previously reported for films prepared from Ti(O^{*i*}Pr)₄, Ti(NO₃)₄, and Ti(tmhd)₂(O^{*i*}Pr)₂ precursors.^{11–13,17,39}

The composition of TiO₂ films has been determined by Rutherford backscattering spectrometry (RBS) measurements as shown in Figure 5(b). The carbon contamination at levels of 1.8–3.5 atom% was estimated using Auger electron spectrometry (AES), which is comparable to those of 3–5 atom% obtained with Ti(tmhd)₂(O^{*i*}Pr)₂ or Ti(tmhd)₂(mpd). A trace amount of carbon is commonly observed in TiO₂ films grown by MOCVD from Ti-alkoxide precursors and could be attributed to the incomplete decomposition of the alkoxide ligand, due to lack of either thermal energy or available oxygen. The carbon contamination levels show a clear dependency on deposition temperatures: 3.5% at 400 °C and 1.8% at 500 °C.

Figure 6(a) and 6(b) show scanning electron microscope (SEM) images of as-deposited film at 450 °C and film annealed at 500 °C, respectively. The formation of densely packed microcrystallites with a grain size of 50–100 nm is clearly seen in Figure 6(b). As the annealing temperature is lowered, a smaller grain size is observed. The fracture cross-section of the film exhibits a columnar structure as depicted in Figure 6(c). There are no humps and hazy appearance on the surface of films grown at all deposition temperatures.

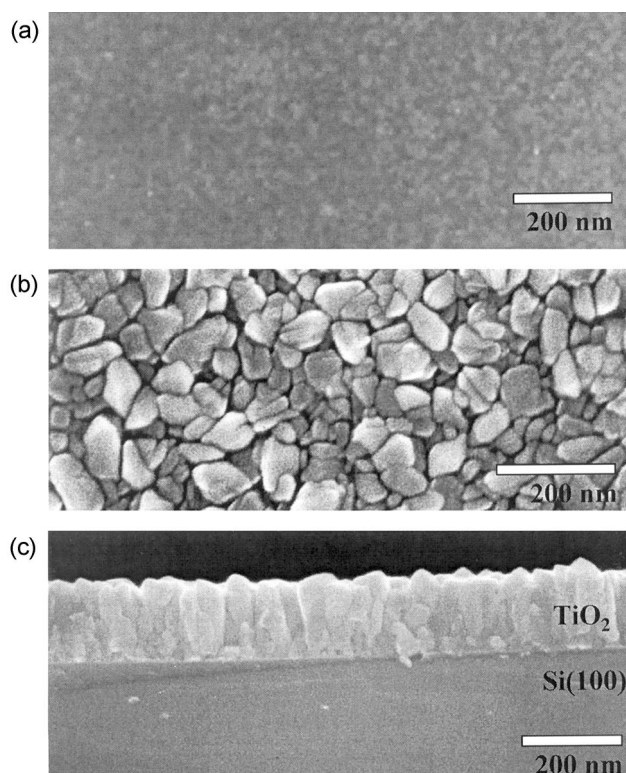


Figure 6. (a) SEM image of TiO₂ film grown at 450 °C; (b) SEM image of TiO₂ film annealed at 500 °C; (c) a cross-sectional view of annealed TiO₂ film on a cleaved Si substrate.

Conclusion

A titanium diisopropoxide compound **1** with β -keto amide ligands has been prepared as MO precursor for the titanate thin films. The structure of this complex in both solid and solution state has been determined by a single crystal X-ray diffraction study and variable-temperature NMR spectroscopy. The thermal behavior of precursor **1** has been examined by thermogravimetry and vapor pressure measurement, revealing an enhanced thermal stability of **1** by introduction of the β -keto amide ligand compared to β -diketonate precursors. Polycrystalline TiO₂ films of pure anatase phase have been deposited on Si(100) by MOCVD after annealing above 500 °C under oxygen. Further studies will concentrate on the compatibility of this β -keto amide titanium precursor for the deposition of thin films of perovskite titanates.

Acknowledgement. This work was supported by the National Research Laboratory (NRL) program of the Korean Ministry of Science & Technology (MOST), the Korea Science & Engineering Foundation (Project No. 1999-1-122-001-5) for J.T.P, and a Korea University Grant for K. L.

References

- Ezhilvalavan, S.; Tseng, T.-Y. *Mater. Chem. Phys.* **2000**, *65*, 227.
- Campbell, S. A.; Gilmer, D. C.; Wang, X.-C.; Hsieh, M.-T.; Kim, H.-S.; Gladfelter, W. L.; Yan, J. *IEEE Trans. Electron Devices* **1997**, *44*, 104.
- Dietz, G. W.; Schumacher, M.; Waser, R.; Streiffer, S. K.; Basceri, C.; Kingon, A. *J. Appl. Phys.* **1997**, *82*, 2359.
- Jones, R. E.; Zurcher, P.; Chu, P.; Taylor, D. J.; Lii, Y. T.; Jiang, B.; Maniar, P. D.; Gillespie, S. J. *Microelectron. Eng.* **1995**, *29*, 3.
- Kang, C. S.; Cho, H. J.; Lee, B. T.; Lee, K. H. *Jpn. J. Appl. Phys.* **1997**, *36*, 6946.
- Peng, C. H.; Desu, S. B. *J. Am. Ceram. Soc.* **1994**, *77*, 1799.
- Rees, W. S. *CVD of Nonmetals*; VCH: Weinheim, 1996.
- Bilodeau, S. M.; Carl, R.; Buskirk, P. V.; Ward, J. *Solid State Technol.* **1997**, 236.
- Kawahara, T.; Yamamuka, M.; Makita, T.; Yuuki, A.; Mikami, N.; Ono, K. *Mat. Res. Soc. Symp. Proc.* **1995**, *361*, 361.
- Hwang, C. S.; Park, S. O.; Cho, H.-J.; Kang, H.-K.; Lee, S. I.; Lee, M. Y. *Appl. Phys. Lett.* **1995**, *67*, 2819.
- Taylor, C. J.; Gilmer, D. C.; Colombo, D. G.; Wilk, G. D.; Campbell, S. A.; Roberts, J.; Gladfelter, W. L. *J. Am. Chem. Soc.* **1999**, *121*, 5220.
- Won, T.; Yoon, S.; Kim, H. *J. Electrochem. Soc.* **1992**, *139*, 3284.
- Takahashi, Y.; Tsuda, K.; Sugiyama, K.; Minoura, H.; Makino, D.; Tsuiki, M. *J. Chem. Soc., Faraday Trans.* **1981**, *77*, 1051.
- Turgambaeva, A. E.; Krisyuk, V. V.; Sysoev, S. V.; Igumenov, I. K. *Chem. Vap. Deposition* **2001**, *7*, 121.
- Ryu, H.; Kim, J. S.; Cho, S.; Moon, S. H. *J. Electrochem. Soc.* **1999**, *146*, 1117.
- Lee, J.; Rhee, S. *Electrochem. Solid-State Lett.* **1999**, *2*, 510.
- Ando, F.; Shimizu, H.; Kobayashi, I.; Okada, M. *Jpn. J. Appl. Phys.* **1997**, *36*, 5820.
- Roeder, J. F.; Vaarstra, B. A.; Van Buskirk, P. C.; Beratan, H. R. *Mater. Res. Soc. Symp. Proc.* **1996**, *415*, 123.
- Beach, D. B.; Vallet, C. E. *Mater. Res. Soc. Symp. Proc.* **1996**, *415*, 225.
- Gardiner, R. A.; Van Buskirk, P. C.; Kirilin, P. S. *Mater. Res. Soc. Symp. Proc.* **1994**, *335*, 221.
- Hong, S. H.; Rim, S. K.; Lee, I.; Min, Y. S.; Kim, D.; Lee, W. I. *Thin Solid Films* **2002**, *409*, 82.
- Min, Y.; Cho, Y. J.; Kim, D.; Lee, J.; Kim, B. M.; Lim, S. K.; Lee, I. K.; Lee, W. I. *Chem. Vap. Deposition* **2001**, *7*, 146.
- Lee, J.; Kim, J.; Shim, J.; Rhee, S. *J. Vac. Sci. Technol. A* **1999**, *17*, 3033.
- Jones, A. C.; Leedham, T. J.; Wright, P. J.; Crosbie, M. J.; Fleeting, K. A.; Otway, D. J.; O'Brien, P.; Pemble, M. E. *J. Mater. Chem.* **1998**, *8*, 1773.
- Hong, S. T.; Lim, J. T.; Lee, J. C.; Xue, M.; Lee, I.-M. *Bull. Korean Chem. Soc.* **1996**, *17*, 637.
- Wolf, W. R.; Sievers, R. E.; Brown, G. H. *Inorg. Chem.* **1972**, *11*, 1995.
- Sheldrick, G. M. *Acta Crystallogr. A* **1990**, *46*, 467.
- Sheldrick, G. M. *Program for the Refinement of Crystal Structures*; University of Göttingen: Germany, 1993.
- Bickley, D. G.; Serpone, N. *Inorg. Chem.* **1976**, *15*, 948.
- Bradley, D. C.; Holloway, C. E. *Chem. Commun.* **1965**, 284.
- Fay, R. C.; Lindmark, A. F. *J. Am. Chem. Soc.* **1983**, *105*, 2118.
- Bickley, D. G.; Serpone, N. *Inorg. Chem.* **1979**, *18*, 2200.
- Bird, P. H.; Fraser, A. R.; Lau, C. F. *Inorg. Chem.* **1973**, *12*, 1322.
- Errington, R. J.; Ridland, J.; Clegg, W.; Coxall, R. A.; Sherwood, J. M. *Polyhedron* **1998**, *17*, 659.
- Williams, P. A.; Jones, A. C.; Wright, P. J.; Crosbie, M. J.; Bickley, J. F.; Steiner, A.; Davies, H. O.; Leedham, T. J. *Chem. Vap. Deposition* **2002**, *8*, 110.
- Jung, O.-J.; Kim, S.-H.; Cheong, K.-H.; Li, W.; Saha, S. I. *Bull. Korean Chem. Soc.* **2003**, *24*, 49.
- Lee, M. S.; Cheon, I. C.; Kim, Y. I. *Bull. Korean Chem. Soc.* **2003**, *24*, 1155.
- Cullity, B. D. *Elements of X-ray Diffraction*; Addison-Wesley: Reading, Mass, 1978.
- Gilmer, D. C.; Colombo, D. G.; Taylor, C. J.; Roberts, J.; Haugstad, G.; Campbell, S. A.; Kim, H.; Wilk, G. D.; Gribelyuk, M. A.; Gladfelter, W. L. *Chem. Vap. Deposition* **1998**, *4*, 9.